small structures
www.small-structures.com

Revealing the 1D Nature of Electronic States in Phosphorene Chains

Maxim Krivenkov, Maryam Sajedi, Dmitry Marchenko, Evangelos Golias, Matthias Muntwiler, Oliver Rader, and Andrei Varykhalov*

Phosphorene, a 2D allotrope of phosphorus, is technologically very appealing because of its semiconducting properties and narrow bandgap. Further reduction of the phosphorene dimensionality may spawn exotic properties of its electronic structure, including lateral quantum confinement and topological edge states. It is demonstrated that dispersions measured along and perpendicular to the phosphorene chains self-assembled on Ag(111) reveal pronounced electronic confinement resulting in a 1D band, flat and dispersionless perpendicular to the chain direction in momentum space. Density functional theory calculations reproduce the 1D band for the experimentally determined structure. It is shown that phosphorene chains aligned equiprobably to three $\langle 1\bar{1}0 \rangle$ directions of the Ag(111) surface can be characterized by angle-resolved photoemission spectroscopy because the three rotational variants are separated in the angular domain. A semiconductor-to-metal phase transition is predicted upon increasing the density of the chain array, a promising approach to band structure engineering.

1. Introduction

Since the first experiments with exfoliated graphene, the field of 2D quantum materials is in the expansive spotlight of fundamental and applied research. Postgraphene 2D materials are formed not only by group IV elements, but also group V, where the latter demonstrate semiconducting properties: prominent examples are bismuthene[1] and recently synthesized arsenene.[2] One of the most intriguing elements of this type is phosphorus and its allotropes, revealing diversity of novel electronic and optical properties.[3] There are several structural polymorphs such as red, green, and blue phosphorus. Black phosphorus (BlackP) is the most stable one, it is a layered material composed of buckled honeycomb sheets of P atoms, held together by van der Waals interaction.[4–7] The tunability of the bandgap in BlackP in wide range (0.3–2.0 eV), combined with high carrier mobility, makes BlackP a perspective material for electronic design[8] and it has already given promising results in transistor and optoelectronic devices.[9,10] However, BlackP is difficult to grow epitaxially, therefore, the mechanical/liquid exfoliation techniques used to produce few- and single-layer BlackP limit the bottom-up approach that is needed for integrated circuit development.

Another 2D polymorph with structural and electronic similarities to monolayer BlackP is the blue phosphorene (BlueP). So far formation of BlueP-like structures has been mainly reported on noble metal substrates.[11–17] In contrast to the bulk and bulk exfoliated systems, epitaxially grown 2D materials cannot easily be characterized optically, in particular when grown on metals substrates. Hence, the discovery of BlueP proceeded in two steps. At first, the candidate material monolayer P/Au(111) has been investigated structurally by scanning tunneling microscopy (STM).[11,12] In a second step, angle-resolved photoemission spectroscopy (ARPES) investigated the band dispersion and confirmed the bandgap of ≈1.1 eV of BlueP.[18,19] However, later experiments demonstrated that the structure of P/Au(111) is rather a network of small BlueP patches connected with Au atoms.[20,21]

A major further step in the design and control of electronic structure of phosphorus would be further reduction of phosphorene dimensionality. Theory predicts that 1D P should host a plethora of interesting phenomena, including giant Stark effect[22] and strain-induced topological phase transition.[23] It is, however, difficult to produce 1D atomic chains and also nanowires from 2D materials since their basis is their weak perpendicular but strong lateral interaction. Nevertheless, nanoribbons have been produced successfully from graphene,[24] TMDCs[25] and phosphorene.[26–28] Non-Fermi liquid behavior has been studied in quasi-1D chains.[29] Recently, CuTe zigzag chains have been realized.[30]

M. Krivenkov, M. Sajedi, D. Marchenko, O. Rader, A. Varykhalov
Helmholtz-Zentrum Berlin für Materialien und Energie
Elektronenspeicherring BESSY II
Albert-Einstein-Str. 15, 12489 Berlin, Germany
E-mail: maxim.krivenkov@helmholtz-berlin.de

E. Golias
MAX IV Laboratory
Lund University
Fotongatan 2, 22484 Lund, Sweden

M. Muntwiler
Center for Photon Science, Paul-Scherrer Institut
5232 Villigen, Switzerland

The ORCID identification number(s) for the author(s) of this article can be found under https://doi.org/10.1002/sstr.202500458.

DOI: 10.1002/sstr.202500458

It was shown that phosphorus on Ag(111) can self-assemble into 1D atomic chains with an armchair structure.[31] Band structure of an equidistant array of such chains was studied by microfocused ARPES.[31] Dispersing bands were observed in the direction perpendicular to the chains, which was interpreted as evidence that phosphorus chains form a 2D network, i.e., they exhibit non-negligible lateral interactions.[31] It should be noted that there are not many cases for metallic 1D systems where the electronic confinement to 1D on the surface could be proven by ARPES, most notable ones are nanowires of Au on stepped Si(111),[32,33] In,[34,35] and Pb[36,37] on Si(111), Tb on Si(110),[38] Bi/Ag(110),[39] Au/Ni(110),[40] and a special case of Bi(441) where two 1D surface-localized states were observed.[41]

Due to the small size of structural domains even applying microfocused ARPES (at the cost of technical complexity and lower intensity compared to conventional ARPES) does not guarantee to capture a single local domain of the structure. In the present work, we use conventional ARPES and demonstrate that atomic chains of P on Ag(111) exhibit very pronounced and perfectly 1D electronic structure. Phosphorus bands disperse between 3 and 1.5 eV binding energy (E_B) in the direction along the chains, but remain extraordinary flat (within 20 meV) in the direction perpendicular to the chains at any E_B. This result is accurately confirmed by density functional theory (DFT) calculations. Using DFT, we also study the evolution of the phosphorus bands with changing separation between P chains, and find a 1D → 2D electronic structure transition for marginally separated chains, which renders them a 2D metal.

Information on experimental techniques and DFT calculations is provided in the Supporting Information.[42]

2. Results and Discussion

Figure 1a,b display characterization of P chains on Ag(111) by STM at moderate P coverage (≈0.6 ML) and at different length scales. P forms mainly 1D structures; however, there are some small 2D islands with lattice rotated by 30° relative to the chains. Figure 1c shows a 3D closeup of the chains, which reveals their armchair atomic structure. From STM images, one sees that P chains are aligned along three equivalent orientations with a mutual angle of 120° between them. These orientations

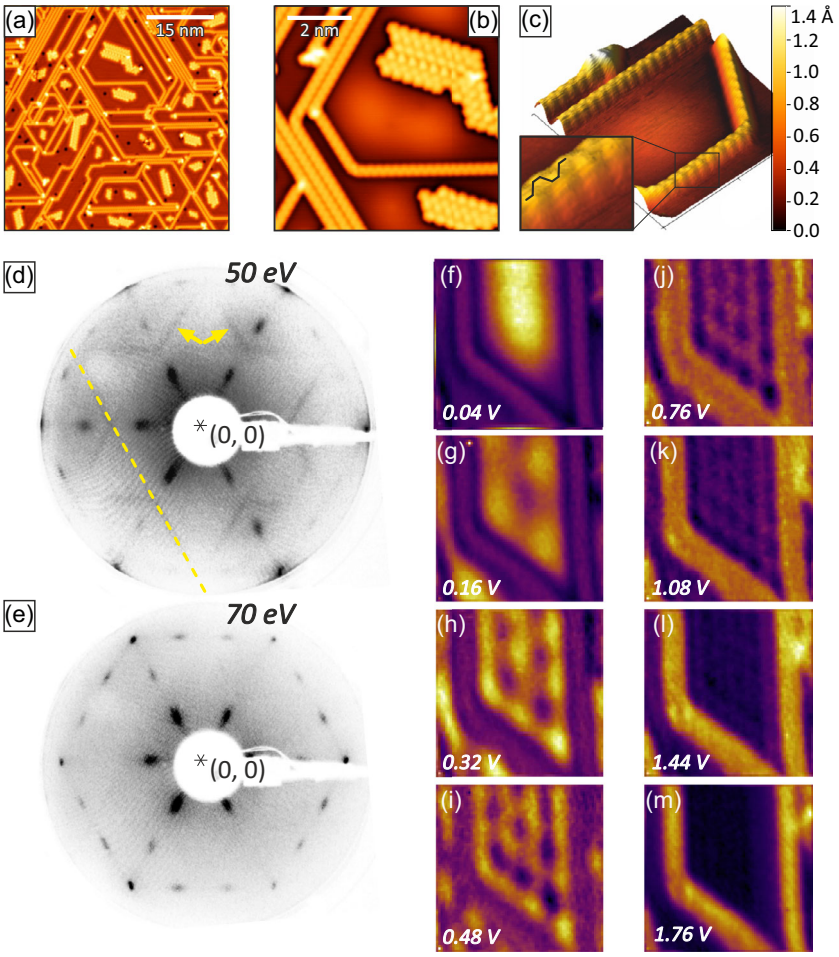

Figure 1. a,b) STM images of 1D P/Ag(111) with small islands of the 2D phase and c) closeup showing armchair-type internal structure of chains ($8 \times 8\,nm^2$). d,e) LEED and f–m) STM/STS characterization of P chains on Ag(111): $\frac{dI}{dV}$ maps showing electronic standing waves of Ag(111) SS in the potential well of P chains; tunneling parameters: (a) −1.0 V, 0.1 nA; (b) −0.1 V, 1.0 nA; and (c) −0.1 V, 3.0 nA.

correspond to the $\langle 1\bar{1}0 \rangle$ family of directions of Ag(111). The formation of three orientational domains of P chains is also confirmed by low-energy electron diffraction (LEED; Figure 1d,e). The displayed LEED patterns correspond to a sample with high P coverage, similar to the sample that was used for ARPES measurements. The LEED reveals a (2×3) pattern which is a superposition of three equally intense (3×1) superlattices and weak (1×2) lines (marked by arrows and dashed line), corresponding to the chains in each of the three domains. The complex appearance of the LEED pattern is discussed in the Supporting Information.[42] In this scenario, the elongation of spots can be explained by an imperfection of chain stacking in the directions perpendicular to the chains. X-ray photoelectron spectroscopy (XPS) spectra of P *2p* and Ag *3d* core levels (Figure S1 of Supporting Information[42]) are in agreement (within 0.1 eV) with Ref. [31]. According to Ref. [31], the fact that Ag *3d* peaks show no chemical shifts as compared to bare Ag implies weak interaction between chains and the substrate and rules out P–Ag surface alloying. We observe only a small shift of Ag *3d* core levels to higher E_B for chains (80 meV) and larger shift (130 meV) for 2D phase of phosphorus on Ag(111) (Figure S1, Supporting Information). The lack of Ag–P surface alloy is indirectly confirmed in scanning tunneling spectroscopy (STS) experiments, in particular $\frac{dI}{dV}$ mapping of the Ag(111) surface state (SS) scattering at P chains. A series of quantum interference patterns (QIP) acquired differentially at various binding energies (bias voltages) is displayed in Figure 1f–m. The real-space periodicity of standing electron waves, converted to momentum space (Figure S6, Supporting Information), allows to determine the *E(k)* dispersion of Ag(111) SS[43,44] laterally confined between P chains. A parabolic fitting of the dispersion provides effective mass $m_{\text{eff}} = (0.46 \pm 0.03)m_0$ and apex energy $E_0 = (3 \pm 18)$ meV. The dispersion was found to be similar to that of the SS at bare Ag(111),[44] except for 50 meV lower binding energy: $m_{\text{eff}} = (0.41 \pm 0.02)m_0$ and $E_0 = (-65 \pm 1)$ meV. This proves that the lateral potential barrier of P chains is so large that the particle-in-a-box model of quantization applies here. This together with our XPS results, which exclude P–Ag surface alloying, demonstrates that there is no leaking of Ag(111) SS into the bulk at the sites of the chains. We conclude that P chains reside on top of Ag(111) and moderately interact with the substrate.

The photoelectrons in ARPES are collected from the whole area illuminated by the photon beam. Even with the use of microfocused ARPES, discerning a signal from a single domain might be very challenging because of the small average size of uniaxially aligned domains. In the present experiment, beam size is on the scale of ≈100 μm. This means that signals from all three orientational domains of P chains are accumulated and superimposed in the ARPES dispersions. For ARPES investigation of 1D structures it is optimal to have them identical and aligned along a single direction in order to be able to clearly separate electronic bands dispersing along the chain and non-dispersing bands of electrons confined in the perpendicular direction.

However, we show below that in the current case conventional ARPES is well applicable for mapping of the 1D electronic structure because the maxima of P valence bands are far away from the center of the surface Brillouin zone (SBZ). As a result, 1D bands of chains with different orientations only partially overlap in **k**-space.

ARPES data was obtained from a sample with high P coverage and it is reflected in the data by the completely suppressed SS of Ag(111) which for a clean surface is located at the $\bar{\Gamma}$ point close to Fermi level (**Figure 2**e). Figure 2a–d report a series of constant energy surfaces (CES) of P chains on Ag(111) extracted from full photoemission mapping I(E,*kx*,*ky*) for different binding energies. Circular-like contours labeled as *Ag-sp* correspond to nearly spherical 3D bulk *sp*-bands of Ag and surface resonances related to them.[45] Electronic states of P chains are seen between *Ag-sp* contours around the $\bar{K}$ point of the Ag(111) SBZ ($\bar{K}_{Ag}$) and are labeled as *P*. They evolve from a cloverleaf-like pattern at $E_B = 2.26$ eV, through crossing straight double lines at $E_B = 1.76$ eV, and to the triangle of single straight lines at $E_B = 1.46$ eV. These lines belong to the 1D band structure of P chains. Every side of the triangle is emitted from one of the chain orientations, as sketched in **Figure 3**a. The overall ARPES dispersion of the band *P* along the direction $\bar{\Gamma} - \bar{K}_{Ag}$ of Ag(111) SBZ (trace T_1 in Figure 2d), which corresponds to the direction along the chains of one of the domains, is depicted in Figure 2e and emphasized by a dashed red line. It has several valleys and shows a pronounced dispersion in a wide energy range between $E_B = 3$ and 1.5 eV. A second band *P′* (marked by a dashed blue line) is a contribution from two other rotated domains sliced at an angle to a high symmetry direction (therefore, it appears stretched along the $k_{\|}$ axis, as compared to P).

The dispersion in Figure 2e reveals the top of chain band *P* at $E_B \approx 1.5$ eV. This shows that the intrinsic bandgap of phosphorene chains is not less than $E_g \approx 1.5$ eV, in agreement with our DFT calculations in **Figure 4**. This result is also supported by our STS data and density of states calculations (see Figure S7 in the Supporting Information).

In contrast to our results, Ref. [31] reports similar dispersions along the chains (with direct interaction between P atoms) and perpendicular to the chains (with a large distance between them). Such results appear unexpected until we suppose observation of rotational domains there. Measurements in $\bar{\Gamma} - \bar{M}_{Ag}$ direction are not optimal for resolving 1D bands from different domains. At the M point two rotated domains cross (Figure 2d). In order to see the 1D band, one needs to look at a slice in k-space where one can resolve the valence band maximum (VBM) of one domain only. For instance, the ARPES slice along the straight line is seen in the CES [trace T_2 in Figure 2d], which is shown in Figure 2f. It reveals perfectly the flat slices of the P band, dispersionless within 20 meV. Signals from other rotational domains (*P′*) are also seen there. The band seen at $E_B \approx 3.5$ eV (white arrows) can be attributed to lower lying P band, which is also predicted by our DFT calculations (see Figure 4d). Due to the (2×3) P/Ag superlattice, the phosphorus BZ fits only six times inside the Ag BZ. The folded VBMs can be repeated but not overlap so much to make bands flat as we observe them in experiment. This excludes a band folding effect on the formation of 1D bands.

A sketch of the 1D band of P chains is shown in Figure 3b. The model of band superposition for three orientational domains is displayed in Figure 3c. This model explains ARPES observations near the $\bar{K}_{Ag}$ point of the Ag(111) SBZ,

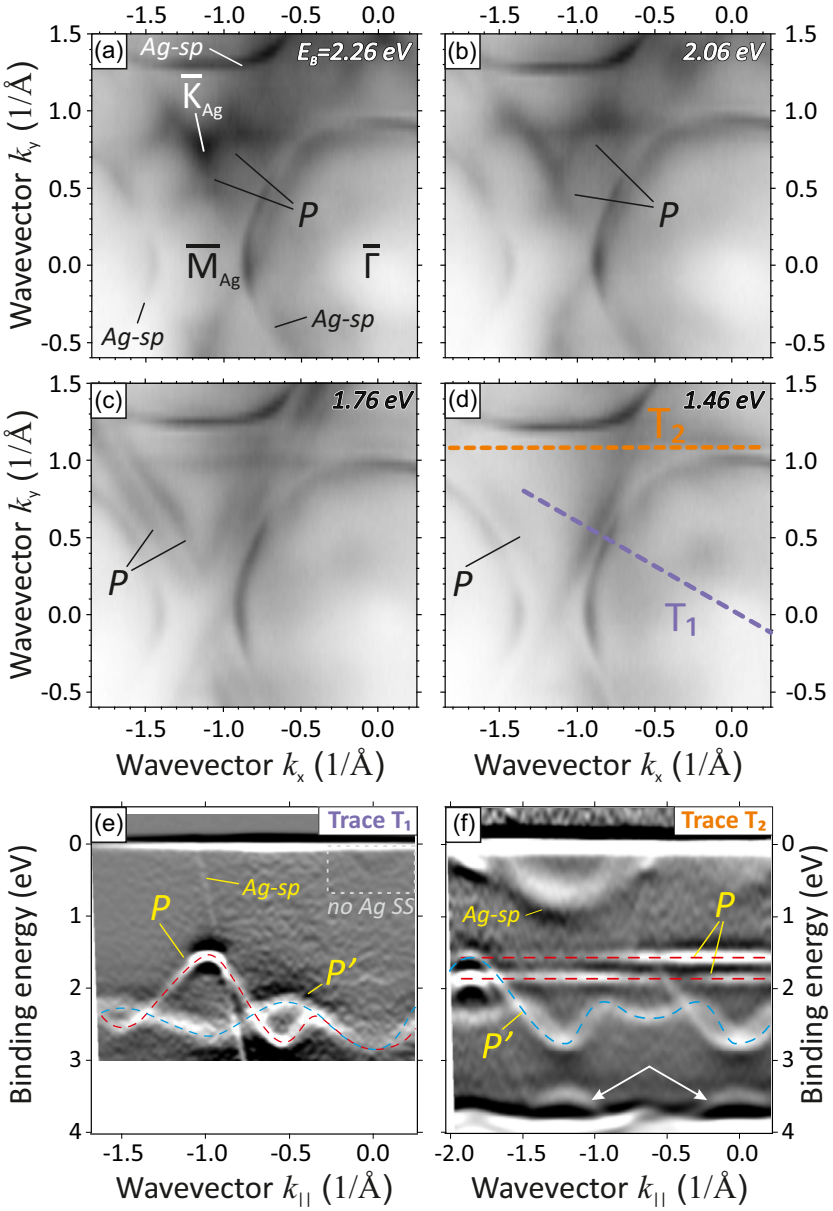

Figure 2. a–d) CES of 1D P on Ag(111) at different binding energies E_B ($h\nu = 80$ eV). Signal from P chains is labeled as *P*, from Ag(111) – as *Ag-sp*; e) dispersion of band *P* along the chains $\left(h\nu = 60\,\text{eV}, \frac{d^2I}{dE^2}\right)$, and f) perpendicular to the chains direction and passing through the *P* valence band maximum $\left(h\nu = 80\,\text{eV}, \frac{dln(I)}{E}\right)$. Contributions from other rotated domains are labeled *P′*. White arrows mark top of the next *P* band.

including the cloverleaf-like pattern at higher E_B and triangular crossings of double and single straight lines at lower E_B. The cross-section on the left side of Figure 3c closely resembles Figure 2f. Additional APRES characterization of this superpositional band structure is reported in the Supporting Information.[42]

We also performed a DFT study of the P chains on Ag(111). The model reproduces the experimentally synthesized chains, resolved by our LEED and STM ((2×3) relative to Ag(111)), and is presented in Figure 4a. The chains are parallel to each other and form a periodic array. This phase corresponds to the high-phosphorus-coverage sample used for ARPES measurements and reflects the structure of a single rotational domain.[31] The overall band structure in the direction $\parallel$ to the chains ($\overline{\Gamma} - \overline{K}_{Ag}$) and $\perp$ to chains (parallel to $\overline{\Gamma} - \overline{M}_{Ag}$, but along the VBM) is shown in Figure 4b,c. A projection on P atoms is presented in Figure 4d,e. Good qualitative agreement with the ARPES experiment is seen, with the characteristic phosphorus band dispersion along the chains and dispersionless character in the direction perpendicular to the chains (see also Figure S2 in the Supporting Information[42]). The electronic structure of P chains is thus confirmed as purely 1D. Using the Bader partitioning method,[46,47] we estimated a charge transfer from the Ag substrate of 0.1e per P atom.

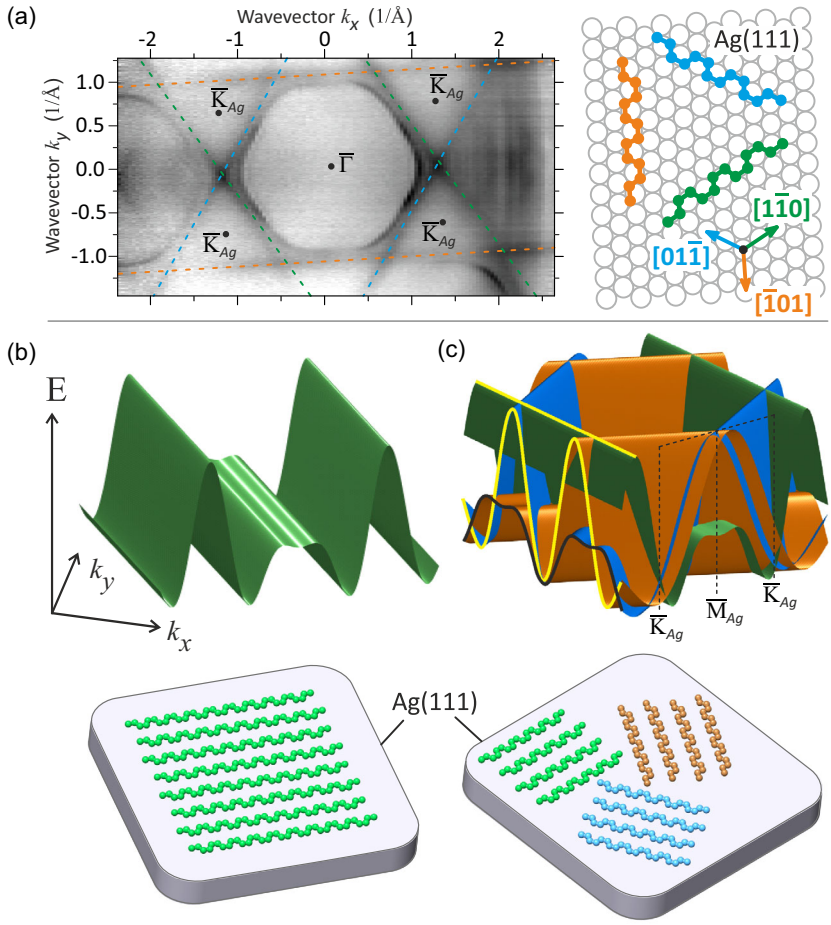

Figure 3. a) Plot explains constitution of the P signal in ARPES and correspondence of straight lines in ARPES map (left) to three orientations of chains (right). ARPES map was measured with $h\nu = 100$ eV and $E_B = 1.51$ eV (top of P band). b) Rough sketch of 1D band of P chains as referred to the orientation of the array of chains. c) Model of superposition of P bands from three orientational domains of phosphorene chains.

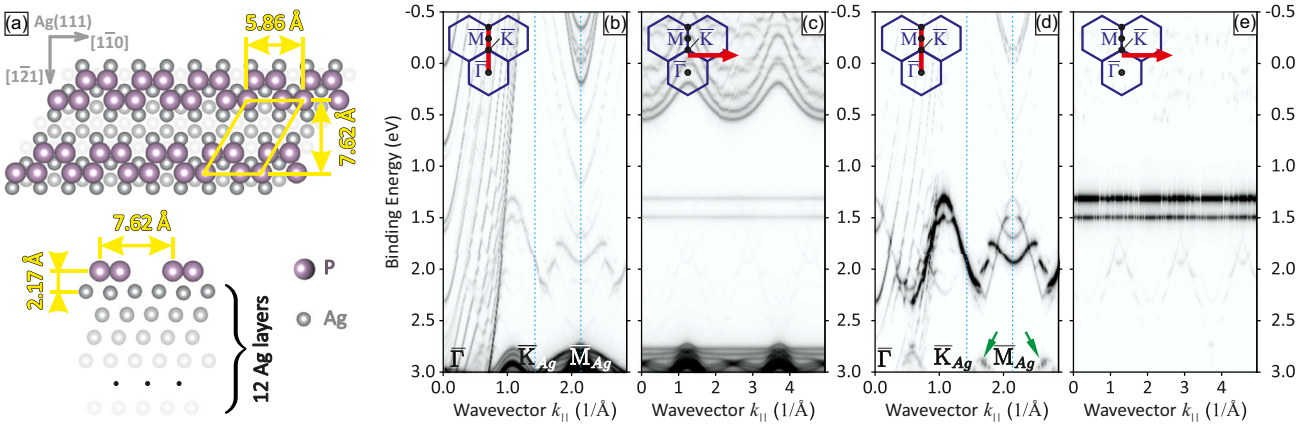

Figure 4. DFT study of P chains; a) Structural model of Ag(111)/*P*-(2 × 3) used in the simulation of experimentally realized chains, top-view (top) and side-view along the chains (bottom); b,c) combined bands of P and Ag; and d,e) projection of the band structure on P atoms. The band structure was calculated along $\overline{\Gamma} - \overline{K}_{Ag}$ of Ag(111) which is parallel to the chains (b,d) and along the perpendicular direction passing through the valence band maximum (c,e). The directions are marked in the insets by red lines. *P*-related bands demonstrate no dispersion perpendicular to the chains in perfect agreement with ARPES experiment. Green arrows in panel (d) mark a lower energy band of P for which a corresponding band is also found in the ARPES data. See Figure S3 and Figure S2 of Supporting Information[42] for DFT plots in a wider energy range and for direct comparison of DFT results to experimental data.

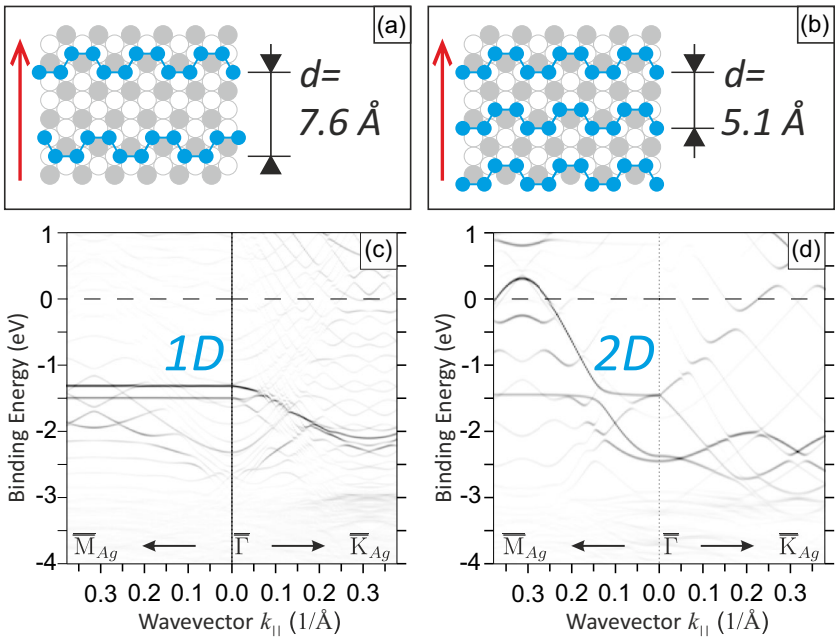

Figure 5. 1D → 2D electronic structure transition upon lateral compression of the chain array; a,b) Atomic model of P chains separated by $d = 7.6$ Å (as in our experiment) and $d = 5.1$ Å (artificially compressed structure) and c,d) calculated electronic band structures projected on P atoms in directions perpendicular (red arrow, $\overline{\Gamma} - \overline{K}_{Ag}$) and parallel ($\overline{\Gamma} - \overline{M}_{Ag}$) to chains. Dispersions are displayed without unfolding.

Furthermore, by DFT, we studied how the band structure of the P chains within the array depends on the lateral separation d between them (**Figure 5**). While the experimentally realized $d = 7.6$ Å (Ag(111)/*P*-(2 × 3)) hosts a 1D P band, a denser simulated array with $d = 5.1$ Å $\left(\text{Ag(111)}/P\text{-}\begin{pmatrix} 2 & 0 \\ -1 & 2 \end{pmatrix}\right)$ triggers interchain interaction and causes a 1D → 2D transition in the electronic structure of the array. The dispersions of the P state calculated for the experimentally synthesized ($d = 7.6$ Å) and for artificial ($d = 5.1$ Å) arrays are compared vis-à-vis in Figure 5c and d, respectively (conducted without unfolding). One sees that in the denser array the P band is not flat but disperses strongly and even crosses the Fermi level (E_F), hence rendering the chains metallic.

Finally, we tested the presence of topological edge states, predicted for the armchair configuration.[48] These states should appear as nearly flat bands in the vicinity of E_F. We found no such bands below E_F in ARPES and no visible signs of them in STS. The absence of topological states can be attributed to their suppression by confinement. According to Ref. [48], the localization of edge states requires a phosphorene nanoribbon with minimal width of 5–6 lattice constants, which is not realized in P chains.

3. Conclusion

In summary, we studied phosphorene atomic chains self-assembled on a Ag(111) substrate in the armchair configuration. Although the chains grow in three equiprobable orientations, aligned to the $\langle 1\bar{1}0 \rangle$ family of directions of Ag(111) rotated by 120° to each other, we show that conventional ARPES can be used for the mapping of their band structure because their bands are separated in the angular domain. We have measured the dispersion of the chain band and show that it is 1D. The band disperses within 1.5 eV along the chain but remains perfectly flat and dispersionless in the direction perpendicular to the chain due to lateral confinement. Our DFT calculations confirm this result and predict a 1D → 2D transition in the electronic structure of the chain array when the lateral separation between the chains is reduced. This transition also changes the band structure of the chains from semiconducting (with intrinsic bandgap $E_g \geq 1.5$ eV) to metallic.

Supporting Information

Supporting Information is available from the Wiley Online Library or from the author.

Acknowledgements

This work was supported by Impuls- und Vernetzungsfonds der Helmholtz-Gemeinschaft under grant no. HRSF-0067. The authors thank the Helmholtz-Zentrum Berlin für Materialien und Energie for the allocation of synchrotron radiation beamtime at the ARPES One-square station. The authors acknowledge the Paul Scherrer Institut, Villigen, Switzerland for provision of synchrotron radiation beamtime at beamline X03DA of the SLS.

Open Access funding enabled and organized by Projekt DEAL.

Conflict of Interest

The authors declare no conflict of interest.

Author Contributions

Maxim Krivenkov: conceptualization (equal); investigation (lead); visualization (equal); writing—original draft (equal); writing—review & editing (lead). **Maryam Sajedi**: conceptualization (supporting); investigation (equal); visualization (supporting); writing—review & editing (equal). **Dmitry Marchenko**: investigation (equal); software (lead); writing—original draft (equal); writing—review & editing (equal). **Evangelos Golias**: conceptualization (lead); investigation (equal); writing—review & editing (equal). **Matthias Muntwiler**: investigation (supporting); writing—review & editing (equal). **Oliver Rader**: supervision (lead); writing—review & editing (equal). **Andrei Varykhalov**: conceptualization (equal); investigation: (equal); supervision (equal); visualization (equal); writing—original draft (lead); writing—review & editing (equal). **Maxim Krivenkov** and **Maryam Sajedi** contributed equally to this work.

Data Availability Statement

The data that support the findings of this study are available from the corresponding author upon reasonable request.

Keywords

1D, angle-resolved photoemission spectroscopy, chains, phosphorus, scanning tunneling microscopy

Received: July 8, 2025
Revised: September 5, 2025
Published online: October 17, 2025

[1] F. Reis, G. Li, L. Dudy, M. Bauernfeind, S. Glass, W. Hanke, R. Thomale, J. Schäfer, R. Claessen, *Science* **2017**, *357*, 287.
[2] J. Shah, W. Wang, H. M. Sohail, R. I. G. Uhrberg, *2D Mater.* **2020**, *7*, 025013.
[3] W. Zhang, X. Zhang, L. K. Ono, Y. Qi, H. Oughaddou, *Small* **2024**, *20*, 2303115.
[4] X. Ling, H. Wang, S. Huang, F. Xia, M. S. Dresselhaus, *PNAS* **2015**, *112*, 4523.
[5] C. Q. Han, M. Y. Yao, X. X. Bai, L. Miao, F. Zhu, D. D. Guan, S. Wang, C. L. Gao, C. Liu, D. Qian, Y. Liu, J.-F. Jia, *Phys. Rev. B* **2014**, *90*, 085101.
[6] F. Xia, H. Wang, J. C. M. Hwang, A. H. C. Neto, L. Yang, *Nat. Rev. Phys.* **2019**, *1*, 306.
[7] E. Golias, M. Krivenkov, J. Sánchez-Barriga, *Phys. Rev. B* **2016**, *93*, 075207.
[8] J. Kim, S. S. Baik, S. H. Ryu, Y. Sohn, S. Park, B.-G. Park, J. Denlinger, Y. Yi, H. J. Choi, K. S. Kim, *Science* **2015**, *349*, 723.
[9] L. Li, Y. Yu, G. J. Ye, Q. Ge, X. Ou, H. Wu, D. Feng, X. H. Chen, Y. Zhang, *Nat. Nanotechnology* **2014**, *9*, 372.
[10] F. Xia, H. Wang, Y. Jia, *Nat. Commun.* **2014**, *5*, 4458.
[11] J. L. Zhang, S. Zhao, C. Han, Z. Wang, S. Zhong, S. Sun, R. Guo, X. Zhou, C. D. Gu, K. D. Yuan, Z. Li, W. Chen, *Nano Lett.* **2016**, *16*, 4903.
[12] W. Zhang, H. Enriquez, Y. Tong, A. Bendounan, A. Kara, A. P. Seitsonen, A. J. Mayne, G. Dujardin, H. Oughaddou, *Small* **2018**, *14*, 1804066.
[13] M. Schaal, J. Picker, F. Otto, M. Gruenewald, R. Forker, T. Fritz, *J. Phys.: Condens. Matter* **2021**, *33*, 485002.
[14] S. Yang, Z. Hu, W. Wang, P. Cheng, L. Chen, K. Wu, *Chin. Phys. Lett.* **2020**, *37*, 096803.
[15] A. Sala, M. Caporali, M. Serrano-Ruiz, F. Armillotta, E. Vesselli, F. Genuzio, T. O. Menteş, A. Locatelli, G. Comelli, C. Africh, A. Verdini, *Nanoscale* **2022**, *14*, 16256.
[16] J. Zhang, X. Dong, S. Xu, Y. Xia, W. Ho, H. Xu, M. Xie, *2D Mater.* **2022**, *9*, 045002.
[17] Y. Kaddar, W. Zhang, H. Enriquez, Y. J. Dappe, A. Bendounan, G. Dujardin, O. Mounkachi, A. El kenz, A. Benyoussef, A. Kara, H. Oughaddou, *Adv. Funct. Mater.* **2023**, *33*, 2213664.
[18] J. Zhuang, C. Liu, Q. Gao, Y. Liu, H. Feng, X. Xu, J. Wang, J. Zhao, S. X. Dou, Z. Hu, Y. Du, *ACS Nano* **2018**, *12*, 5059.
[19] E. Golias, M. Krivenkov, A. Varykhalov, J. Sánchez-Barriga, O. Rader, *Nano Lett.* **2018**, *18*, 6672.
[20] S. Zhao, J. L. Zhang, W. Chen, Z. Li, *J. Phys. Chem. C* **2024**, *124*, 2020.
[21] H. Tian, J.-Q. Zhang, W. Ho, J.-P. Xu, B. Xia, Y. Xia, J. Fan, H. Xu, M. Xie, S. Tong, *Matter* **2020**, *2*, 111.
[22] Q. Wu, L. Shen, M. Yang, Y. Cai, Z. Huang, Y. P. Feng, *Phys. Rev. B* **2015**, *92*, 035436.
[23] E. Taghizadeh Sisakht, F. Fazileh, M. H. Zare, M. Zarenia, F. M. Peeters, *Phys. Rev. B* **2016**, *94*, 085417.
[24] J. Cai, P. Ruffieux, R. Jaafar, M. Bieri, T. Braun, S. Blankenburg, M. Muoth, A. P. Seitsonen, M. Saleh, X. Feng, K. Müllen, R. Fasel, *Nature* **2010**, *466*, 470.
[25] H. E. Lim, Z. Liu, J. Kim, J. Pu, H. Shimizu, T. Endo, Y. Nakanishi, T. Takenobu, Y. Miyata, *ACS Appl. Nano Mater.* **2022**, *5*, 1775.
[26] M. C. Watts, L. Picco, F. S. Russell-Pavier, P. L. Cullen, T. S. Miller, S. P. Bartuś, O. D. Payton, N. T. Skipper, V. Tileli, C. A. Howard, *Nature* **2019**, *568*, 216.
[27] H. Wang, Y. Song, G. Huang, F. Ding, L. Ma, N. Tian, L. Qiu, X. Li, R. Zhu, S. Huang, H. Yan, X. H. Chen, L. Ding, C. Zheng, W. Ruan, Y. Zhang, *Nat. Mater.* **2024**, *23*, 470.
[28] W. Zhang, J. Wang, X. Zhong, X. Zhang, *Small* **2025**, *21*, 2501934.
[29] X. Du, L. Kang, Y. Y. Lv, J. S. Zhou, X. Gu, R. Z. Xu, Q. Q. Zhang, Z. X. Yin, W. X. Zhao, Y. D. Li, S. M. He, D. Pei, Y. B. Chen, M. X. Wang, Z. K. Liu, Y. L. Chen, L. X. Yang, *Nat. Phys.* **2023**, *19*, 40.
[30] J. Gao, H. Cao, X. Hu, H. Zhou, Z. Cai, Q. Zhao, D. Li, Z. Gao, S.-I. Ideta, K. Shimada, P. Cheng, L. Chen, K. Wu, S. Meng, B. Feng, *Phys. Rev. Lett.* **2025**, *134*, 086202.
[31] W. Zhang, H. Enriquez, Y. Tong, A. J. Mayne, A. Bendounan, A. Smogunov, Y. J. Dappe, A. Kara, G. Dujardin, H. Oughaddou, *Nat. Commun.* **2021**, *12*, 5160.
[32] P. Segovia, D. Purdie, M. Hengsberger, Y. Baer, *Nature* **1999**, *402*, 504.
[33] J. N. Crain, A. Kirakosian, K. N. Altmann, C. Bromberger, S. C. Erwin, J. L. McChesney, J.-L. Lin, F. J. Himpsel, *Phys. Rev. Lett.* **2003**, *90*, 176805.
[34] H. W. Yeom, S. Takeda, E. Rotenberg, I. Matsuda, K. Horikoshi, J. Schaefer, C. M. Lee, S. D. Kevan, T. Ohta, T. Nagao, S. Hasegawa, *Phys. Rev. Lett.* **1999**, *82*, 4898.
[35] J. R. Ahn, J. H. Byun, H. Koh, E. Rotenberg, S. D. Kevan, H. W. Yeom, *Phys. Rev. Lett.* **2004**, *93*, 106401.
[36] C. Tegenkamp, T. Ohta, J. L. McChesney, H. Dil, E. Rotenberg, H. Pfnür, K. Horn, *Phys. Rev. Lett.* **2008**, *100*, 076802.
[37] K. S. Kim, H. Morikawa, W. H. Choi, H. W. Yeom, *Phys. Rev. Lett.* **2007**, *99*, 196804.
[38] S. Appelfeller, M. Franz, M. Karadag, M. Kubicki, R. Zielinski, M. Krivenkov, A. Varykhalov, A. Preobrajenski, M. Dähne, *Appl. Surf. Sci.* **2023**, *607*, 154875.
[39] P. M. Sheverdyaeva, D. Pacilè, D. Topwal, U. Manju, M. Papagno, V. Feyer, M. Jugovac, G. Zamborlini, I. Cojocariu, C. Tusche, X. L. Tan, K. Hagiwara, Y.-J. Chen, J. Fujii, P. Moras, L. Ferrari,

E. Vescovo, G. Bihlmayer, C. Carbone, *Phys. Rev. B* **2022**, *106*, 045108.
[40] C. Pampuch, O. Rader, T. Kachel, W. Gudat, C. Carbone, R. Kläsges, G. Bihlmayer, S. Blügel, W. Eberhardt, *Phys. Rev. Lett.* **2000**, *85*, 2561.
[41] M. Bianchi, F. Song, S. Cooil, A. F. Monsen, E. Wahlström, J. A. Miwa, E. D. L. Rienks, D. A. Evans, A. Strozecka, J. I. Pascual, M. Leandersson, T. Balasubramanian, P. Hofmann, J. W. Wells, *Phys. Rev. B* **2015**, *91*, 165307.
[42] Supplementary information is available online.
[43] H. Hövel, B. Grimm, B. Reihl, *Surf. Sci.* **2001**, *477*, 43.
[44] S. Grothe, S. Johnston, S. Chi, P. Dosanjh, S. A. Burke, Y. Pennec, *Phys. Rev. Lett.* **2013**, *111*, 246804.
[45] M. Krivenkov, D. Marchenko, M. Sajedi, A. Fedorov, O. J. Clark, J. Sánchez-Barriga, E. D. L. Rienks, O. Rader, A. Varykhalov, *Nanoscale* **2022**, *14*, 9124.
[46] G. Henkelman, A. Arnaldsson, H. Jónsson, *Comput. Mater. Sci.* **2006**, *36*, 354.
[47] E. Sanville, S. D. Kenny, R. Smith, G. Henkelman, *J. Comput. Chem.* **2007**, *28*, 899.
[48] T. Tani, M. Hitomi, T. Kawakami, M. Koshino, *Phys. Rev. B* **2022**, *105*, 075407.